ISSN 0020-4412, Instruments and Experimental Techniques, 2011, Vol. 54, No. 5, pp. 740–747. © Pleiades Publishing, Ltd., 2011.
Original Russian Text © S.T. Boldarev, R.B. Gusev, S.I. Danilin, A.Ya. Parshin, 2011, published in Pribory i Tekhnika Eksperimenta, 2011, No. 5, pp. 149–156.

LABORATORY TECHNIQUES

Use of a Quartz Resonator of the Tuning Fork Type as a Thermometer in a Dilution Refrigerator

S. T. Boldarev, R. B. Gusev, S. I. Danilin, and A. Ya. Parshin

Kapitza Institute for Physical Problems, Russian Academy of Sciences, ul. Kosygina 2, Moscow, 119334 Russia
Moscow Institute of Physics and Technology, Institutskii per. 9, Dolgoprudnyi, Moscow oblast, 141700 Russia

Received April 4, 2011

Abstract—The temperature dependences of the resonance frequency and resonance width of a tuning-fork-type quartz resonator, which is placed directly in the dilution chamber of a refrigerator, were measured in order to test the possibility of using it as a secondary thermometer under such conditions. Measurements were performed both in the upper and lower phases of a stratified solution of ^{3}He in ^{4}He in the temperature range 15–350 mK. The dependences obtained indicate that the parameters of resonators depend on not only the temperature, thus making it problematic to use them for thermometry in a cryostat's dilution chamber.

DOI: 10.1134/S0020441211050101

INTRODUCTION

In studies of the properties of liquid ^{3}He and ^{4}He and their solutions, quartz tuning forks (QTFs) are widely used (Fig. 1). They are batch-produced for obtaining frequency standards in electronics and are commercially available in the form that is almost ready for use in low-temperature applications: it will be necessary only to open a vacuum metal shell or to completely remove it. Quartz resonators are easily mounted. They are used as fast and precise temperature and pressure sensors in pure ^{3}He and ^{4}He and in diluted solutions of ^{3}He in ^{4}He. The main advantage of QTFs in comparison to the resistance thermometers is their insensitivity to electromagnetic pickups.

The specific features of operation of QTFs in pure ^{3}He and ^{4}He and in diluted solutions of ^{3}He in ^{4}He were studied in [1–3]. The resonator parameters depend on the properties of the environment, mainly on the viscosity η and density ρ. The resonance width is proportional to the value of $\rho\delta$, where $\delta = \sqrt{2\eta/\rho\omega}$ is the viscous penetration depth, and the resonance frequency shift is proportional to the associated liquid

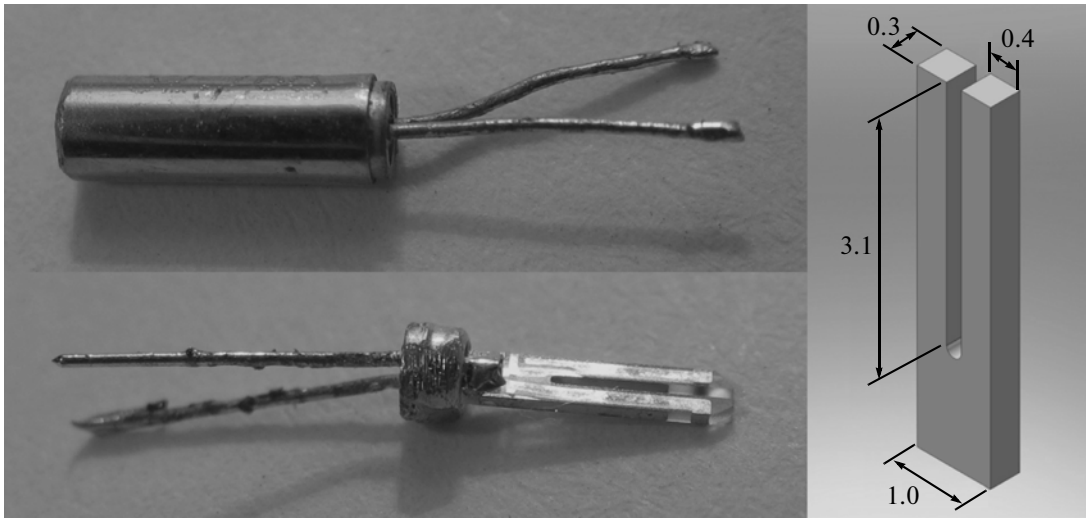

Fig. 1. Quartz tuning fork in a metal case and without it. The dimensions of the QTF used in the experiments are presented on the right.

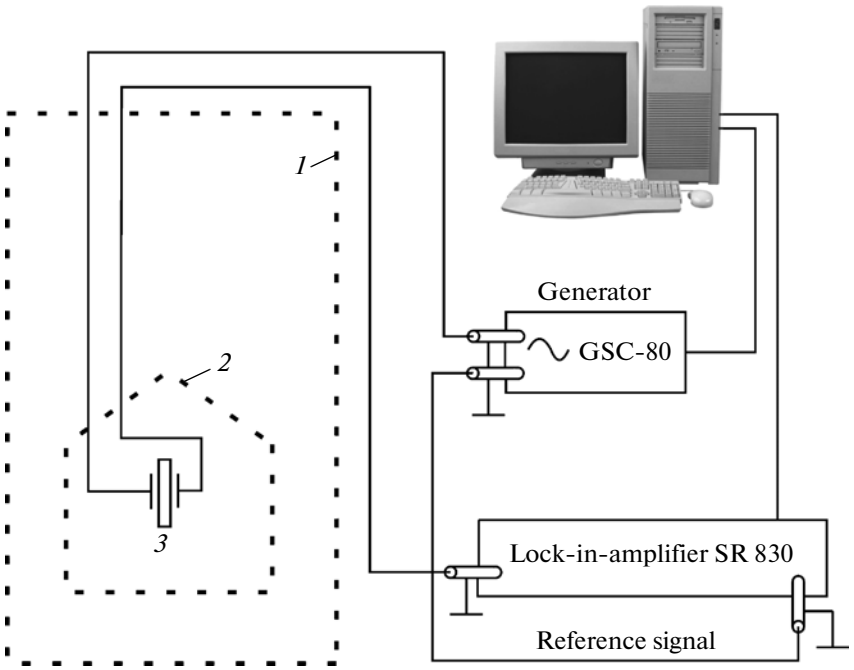

Fig. 2. Measurement scheme: (*1*) vacuum jacket, (*2*) dilution chamber, and (*3*) quartz tuning fork.

mass that depends on its density, resonator geometry, and penetration depth [1]. As was noted in [1], the temperature dependences of the resonance parameters and the widths of the resonance curves for QTFs in vacuum, which belong to the same experimental series, may appreciably differ from one another. Therefore, each particular QTF must be calibrated, and then it can be used as a pressure sensor or a secondary thermometer. The strong temperature dependence of the viscosity of pure ^{3}He and solutions of ^{3}He in ^{4}He at $T < 100$ mK ensures a sufficient sensitivity of such a thermometer.

It is technologically convenient to place a QTF directly in the dilution chamber of a refrigerator because this design does not require manufacturing of additional helium-filled cells. However, a QTF was used as a sensor in the dilution chamber only in [1], where a plot of the time dependence of the QTF resonance width for the cryostat cooling process is presented, but these data were not analyzed. In connection with this, it is of interest to check the possibility of using a QTF as a secondary thermometer, which is placed directly in a refrigerator's dilution chamber. This was the objective of the presented study.

Two experimental runs were performed. In the first and second runs, the QTF was positioned in the upper (concentrated) and lower (diluted) phases of the stratified solution in the cryostat dilution chamber, respectively.

MEASUREMENT TECHNIQUE

The measurement scheme is shown in Fig. 2. The components (orthogonal I_d and in-phase I_a) of a current flowing through the QTF were measured using a phase-sensitive detector (PD) (SR830 lock-in amplifier). An exciting voltage was fed from a GSS-80 generator, which also specified a synchronization signal for the PD.

When the QTF was placed in the lower phase, a current-to-voltage converting SR570 preamplifier was installed in front of the PD. The PD was tuned to the operation in a potential mode and measured the voltage at the preamplifier output. The preamplifier was placed near the cryostat cap. This minimized the effective length of the measuring line from the QTF to the PD, thus reducing the loss in this line and allowing the quality factor to be increased.

Signals were transmitted via 50-Ω coaxial cables from the cryostat to the generator and PD. There was a flange with two hermetically sealed lead-ins on the vacuum jacket. A measuring line in the form of thin PK-50-0.6-23 coaxial cables, which were placed directly in liquid helium, was laid between these lead-ins and the cryostat cap. The connectors were sealed with an epoxy resin. To reduce the parasitic capacitance inside the vacuum jacket, the measuring line was manufactured from two superconducting wires (~0.1 mm in diameter) that were pasted with the БФ-2 adhesive ~3 mm apart on a cigarette paper strip ~5 mm wide. The length of the resulting strip was

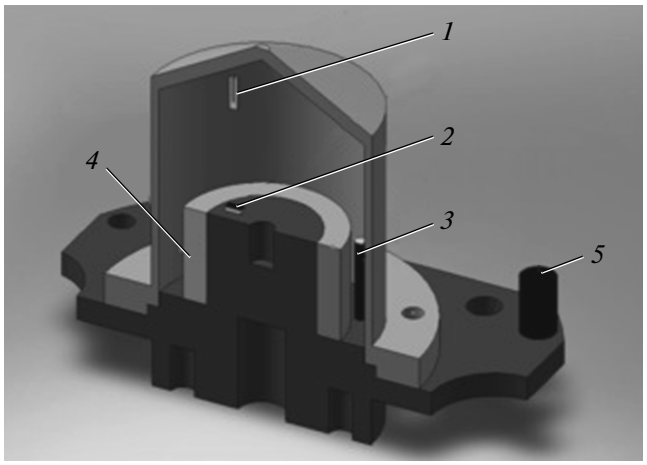

Fig. 3. Dilution chamber of the cryostat: (*1*) quartz tuning fork, (*2*) resistance thermometer, (*3*) internal heater, (*4*) heat exchanger of sintered silver, and (*5*) external heater.

~30 cm, its capacitance was ~4.8 pF, and the resistance of each wire at room temperature was 11.5 Ω.

In the described case, the current components can be represented in the form

$$I_d = \frac{I_0}{2}\frac{\frac{\Delta f}{2}\cos\varphi + (f - f_0)\sin\varphi}{\left(\frac{\Delta f}{2}\right)^2 + (f - f_0)^2}, \quad (1)$$

$$I_a = \frac{I_0}{2}\frac{\frac{\Delta f}{2}\sin\varphi - (f - f_0)\cos\varphi}{\left(\frac{\Delta f}{2}\right)^2 + (f - f_0)^2}, \quad (2)$$

where I_0 is a dimensional constant, Δf is the absorption curve width, f_0 is the resonance frequency, and φ is the phase incursion in the measuring line. If $\varphi = 90°$ in expressions (1) and (2), the resonance curves at the condition $\Delta f << f_0$ take on a usual Lorentzian form.

The resonance frequency and the resonance width were determined by two methods. In the first one, the frequency dependences of the orthogonal and in-phase current components were measured. A typical time that was necessary for such measurements was at least 10–30 min. Such a long time is inconvenient. In the second method, the same current components were recorded as functions of time at a fixed excitation frequency that was close to the resonance frequency. If the current components measured at a single frequency are known and it is assumed that the resonance curves have Lorentzian profiles, the resonance frequency and width can be determined from formulas (1) and (2). This makes it possible to obtain a virtually continuous (the time interval between successive measurements was ~2 s) time dependence of the QTF resonance parameters during the operation of the dilution cryostat.

Figure 3 shows the arrangement of the measuring elements inside the dilution chamber. QTF *1* with the removed metal case is shown in the position that was used in the first experimental run (the vertical orientation of the QTF legs in the upper part of the chamber). In the second run, the QTF was positioned horizontally at a height of 7–8 mm from the upper edge of heat exchanger *4*. In addition to the QTF, RuO_2 resistance thermometer *2* and heater *3* were also placed in the refrigerator's dilution chamber. Another heater *5* was outside the dilution chamber on the copper plate of its base. Both heaters were manufactured from a manganin ($R \approx 100\ \Omega$).

RESULTS AND DISCUSSION

Two different QTFs from a common batch were used in two experimental runs. The values of the resonance curve width and the resonance frequency of the QTF, which was used in the concentrated phase, are $T \approx 11.4$ Hz and $f_0 \approx 32702$ Hz, respectively. The resonance curve of the QTF that operated in the diluted phase was measured in vacuum at $T \approx 4.8$ K with and without using a preamplifier and had widths of ~0.37 and ~0.06 Hz, respectively. The resonance frequency for this QTF is $f_0 \approx 32709$ Hz.

The power released by the QTF in liquid helium at a voltage amplitude of 5 mV, which was used in the experiments, was within 50 pW, thus guaranteeing the absence of noticeable overheating of such a thermometer by the measuring current. The vibration amplitudes of the QTF legs in vacuum and liquid helium are ~1 μm and ~30 nm, respectively.

MEASUREMENTS IN THE CONCENTRATED PHASE

The width of the resonance curve and the resonance frequency in the upper phase were measured using the first method. It was revealed that the QTF parameters are appreciably influenced not only by the temperature but also by other characteristics of the process: the direction and rate of temperature changes and the position of the QTF relative to the stratification boundary (Fig. 4).

In addition, along with resonances with an ordinary Lorentzian profile (Fig. 5), dependences of more complex form that indicate the onset of spontaneous vibrations were also recorded, during which the medium parameters periodically change with a characteristic time of tens of seconds.

These vibrations are directly detected when a signal is recorded as a function of time at a fixed excitation frequency (Fig. 6).

Experiments were also performed in which short (~5 s) heat impulses were fed from the internal of external heater during recording of the current components.

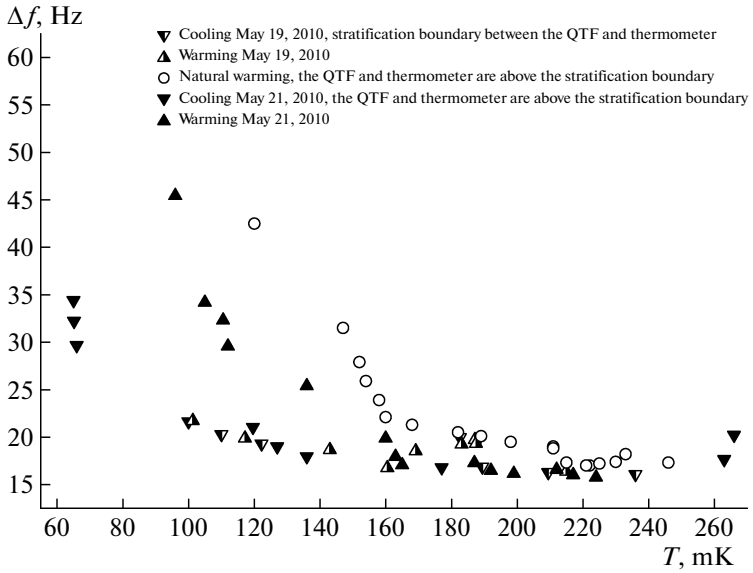

Fig. 4. Data on the widths of the resonance curves obtained for the QTF placed in the concentrated phase.

Simultaneously, the resistance of the thermometer that was in the dilution chamber was recorded (every 50 s) (Fig. 7). Before the heat impulses were fed, the temperature in the dilution chamber in this experiment was ~60 mK. In this temperature region, the upper phase is actually pure ^{3}He whose viscosity increases with a decrease in the temperature ($\sim 1/T^2$) and the resonance width correspondingly increases.

The first heat impulse was fed at time moment *1* and terminated at time moment *2*. In Fig. 7d, the time is a parameter. The values of the resonance frequency and width that correspond to the same moment were obtained from the time dependences of the current components. Figure 7 shows that a heat impulse causes warming of the dilution chamber, which is detected by the resistance thermometer, and simultaneously, despite expectations, leads to an increase in the resonance width (*1* ⟶ *2*). After the impulse terminates, the system returns to the initial state (*2* ⟶ *3* ⟶ *1*).

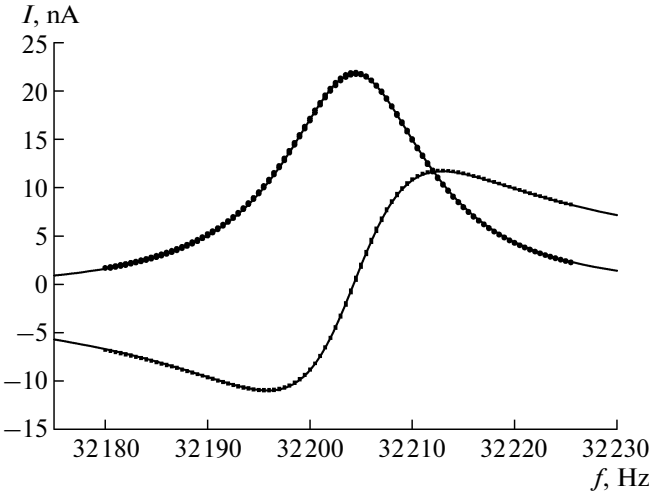

Fig. 5. Resonance curves of ordinary Lorentzian profile at $T \approx 165$ mK.

The cause of such an anomalous behavior of the resonator can be associated with the presence of a superfluid film of the lower phase that covers all solid surfaces inside the dilution chamber, which are above the stratification boundary [4], including the resonator surface.

The influence of this film on the resonator characteristics can be quite appreciable if the film thickness is comparable with the viscous penetration depth, which changes from ~1.5 to ~15 μm in the temperature range from 100 to 10 mK. The film thickness on a smooth surface is 20–30 nm. However, as is seen in a high-resolution photograph of an analogous QTF [3], a typical size of QTF surface irregularities is several microns. The radius of the surface curvature of a film that coats the QTF, which is positioned at a height $h = 1$ cm above the stratification boundary, is determined by the surface tension [5] and can be evaluated at ~8 μm. Because the radius of curvature is comparable with the characteristic roughness size, the average film thickness occurs to be of the same order of magnitude as the characteristic roughness size, i.e., several microns.

A satisfactory description of the influence of the film thickness on the resonator characteristics can be obtained within the framework of the following simple model. Let Δ_3 and Δ_4 be the widths of the resonance curves in the upper and lower phases, respectively, δ be the viscous penetration depth, and d be the film thickness. Assuming that the contribution of the lower

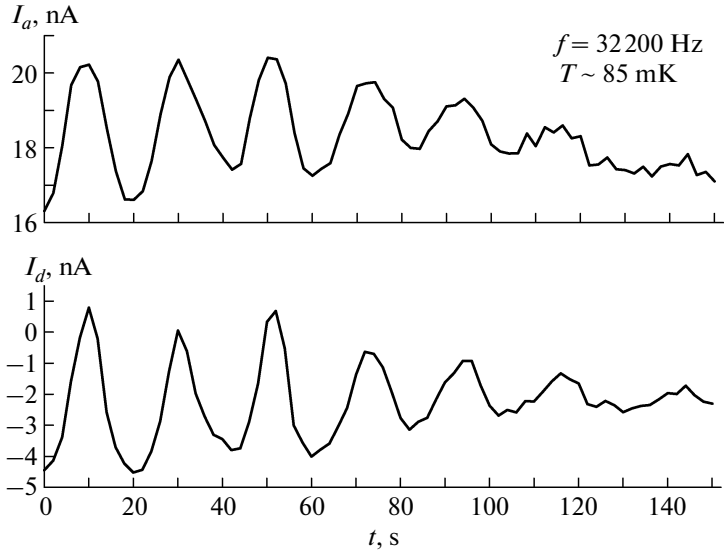

Fig. 6. Spontaneous oscillations arising in the system.

phase to the resonance width is proportional to the film thickness, this width can be represented in the form

$$\Delta = \frac{\Delta_4 d}{d+\delta} + \frac{\Delta_3 \delta}{d+\delta} = \Delta_3 - (\Delta_3 - \Delta_4)\frac{d}{d+\delta}. \quad (3)$$

When considering the dependence of the resonance frequency on the film thickness, two effects must be taken into account: replacement of light ^{3}He with heavier ^{4}He and a decrease in the resonance frequency associated with the viscosity. Let f_{30} and f_{40} be the resonance frequencies for pure ^{3}He and ^{4}He without account for the viscosity, l is the characteristic linear size of the QTF, and B is a numerical factor that depends on the geometrical shape of the QTF. If both effects are taken into account, the resonance vibration frequency can be represented as

$$f_0 = f_{30} - \frac{B\delta^2}{d+\delta} - \frac{f_{30} - f_{40}}{l} d. \quad (4)$$

The following designations are introduced: $\tilde{f} = f_0 - (f_{30} - B\delta)$, $\tilde{\Delta} = \Delta - \Delta_3$. From Eqs. (3) and (4), the dependence $\tilde{f}(\tilde{\Delta})$ is obtained:

$$\tilde{f} = \frac{-\frac{B\delta}{\Delta_3 - \Delta_4}\tilde{\Delta}^2 + \left(\frac{(f_{30} - f_{40})\delta}{l}\right)\tilde{\Delta}}{\tilde{\Delta} + (\Delta_3 - \Delta_4)}. \quad (5)$$

The experimental data presented in Fig. 7d can be approximated with this dependence (Fig. 8). Using the values of the coefficients $B\delta$, $(\Delta_3 - \Delta_4)$, and $(f_{30} - f_{40})\delta/l$ resulting from the approximation, we obtain that the ratio d/δ may be both below and above 1; thus, the film thickness is really comparable with the viscous penetration depth.

In addition, temperature gradients in the dilution chamber may significantly affect the thickness of the QTF-coating film of the lower phase. To evaluate the temperature difference between the interphase boundary and the QTF that is required for the formation of a macroscopic lower-phase droplet on the QTF surface, which is positioned at a height $h = 1$ cm above the interphase boundary, let us write the equilibrium equation for the superfluid component of the lower phase:

$$(\rho_4 - \rho_c)gh = \Delta\Pi_{\text{osm}} + \frac{1}{v_4}\int_0^h s_4 dT,$$

where ρ_4 and ρ_c are the densities of ^{4}He and the concentrated phase, respectively; $\Delta\Pi_{\text{osm}}$ is the difference of osmotic pressures; and v_4 and s_4 are the ^{4}He volume and entropy per atom, respectively. The second term on the right-hand side of the equation is the flowing pressure, which is much lower than the difference of osmotic pressures, and thus can be ignored. For $\Delta\Pi_{\text{osm}} \approx 120\Delta T$ Torr [6, p. 185, Fig. 5.17] and $(\rho_4 - \rho_c)gh \approx 0.05$ Torr, we obtain $\Delta T \approx 0.4$ mK. The appearance of such and larger temperature gradients in the operating setup is quite probable because of the low thermal conductivity of the upper phase (~70 μW/(cm K) [7, p. 28]) in which the QTF is placed. The presence of a temperature gradient causes a flow of the superfluid component over the film, which is sometimes accompanied by self-excited oscillations [4]. Evidently, exactly this type of oscillations was observed in our experiments (Fig. 6). As to the response of the QTF to heat impulses, these, by raising the temperature of the lower phase, make the film thinner, thus increasing the resonance-curve width according to formula (3).

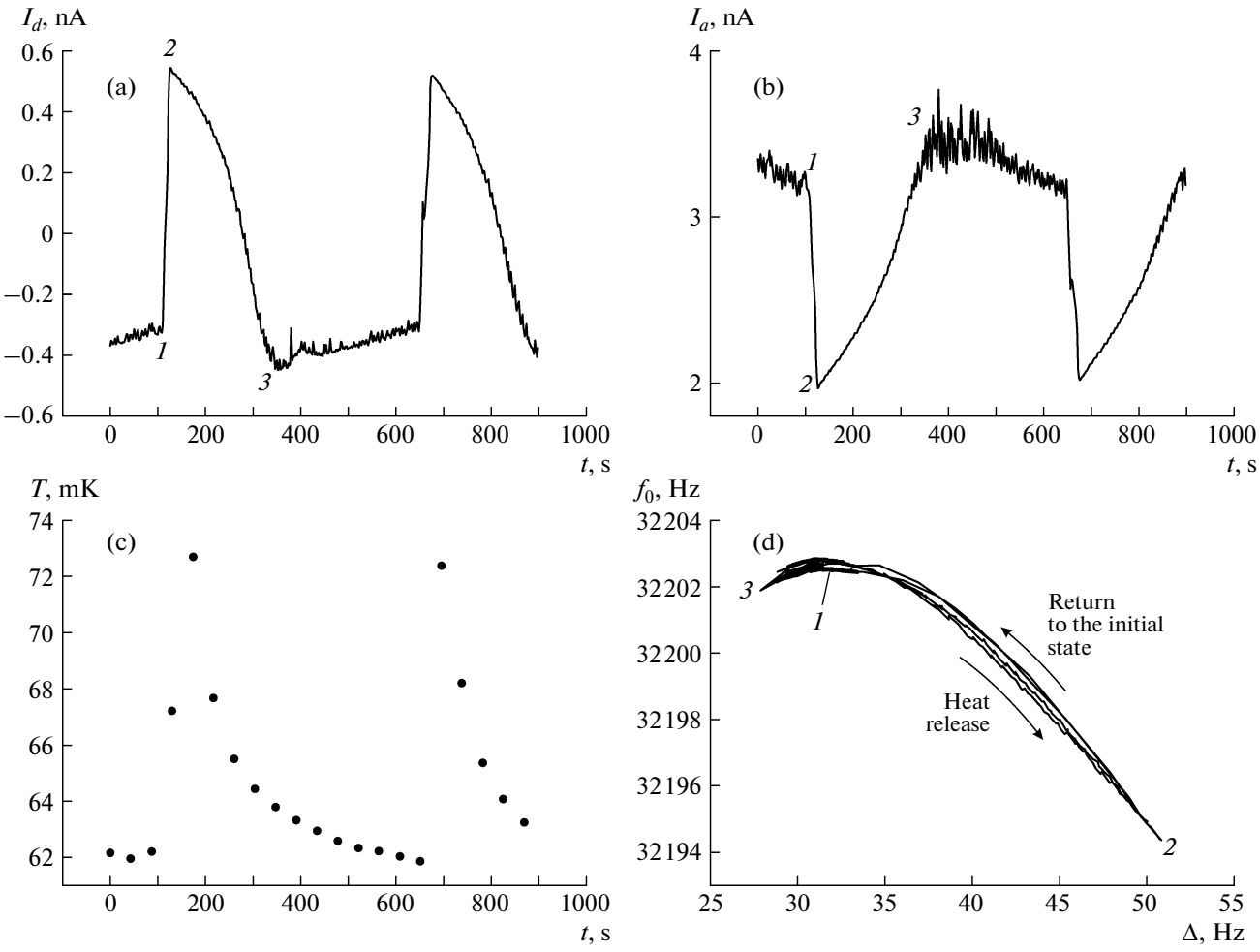

Fig. 7. Response of the QTF to heat impulses: (a) orthogonal and (b) in-phase current components, (c) time-dependent readings of the resistance thermometer, and (d) resonance frequency as a function of the resonance-curve width.

MEASUREMENTS IN THE LOWER PHASE

In a run of experiments in the lower phase of the solution, another QTF from the same batch was used. In these experiments, measurements were performed mainly by the second method, in which the voltage components were recorded as function of time at a constant excitation frequency. From time to time, the shape of the resonance curves was monitored. This shape was used to determine the values of I_0 and φ (see (1) and (2)), which are necessary in calculations of $\Delta(t)$ and $f_0(t)$, and to correct the frequency at which the time record was performed. The readings of the resistance thermometer in the dilution chamber were recorded synchronously with the voltage components.

Figure 9 shows the temperature dependences of the resonance width and frequency. The general form of the curves allows one to conclude that the resonance parameters of the QTF in the lower phase can be used for rough determination of the temperature. At $T >$ 100 mK, the resonance frequency is more temperature-sensitive, and the resonance-curve width is more sensitive at lower temperatures.

Multiple peaks in the curve $\Delta(T)$ at $T > 100$ mK are most likely related to the second-sound resonances that a similar to those observed in [2]. The authors of [2] used capsulated QTFs with open but not removed cylindrical cases. The peaks observed in this study were explained by the appearance of second-sound resonances in gaps between the walls of the case and the QTF legs. In our experiments, the cylindrical case was completely removed and the distance between the QTF to the nearest wall of the dilution chamber (7–8 mm) was almost 20 times larger than the second-sound wavelength at a frequency of ~32 kHz (~0.4 mm at 100 mK). Therefore, only the linear dimensions of the QTF are the geometrical parameters comparable with the wavelength.

Apart from this, a systematic shift in the widths of the resonance curves is observed at $T = 75$–140 mK. This shift may be related to different temperature gradients in the considered processes (the cooling rates

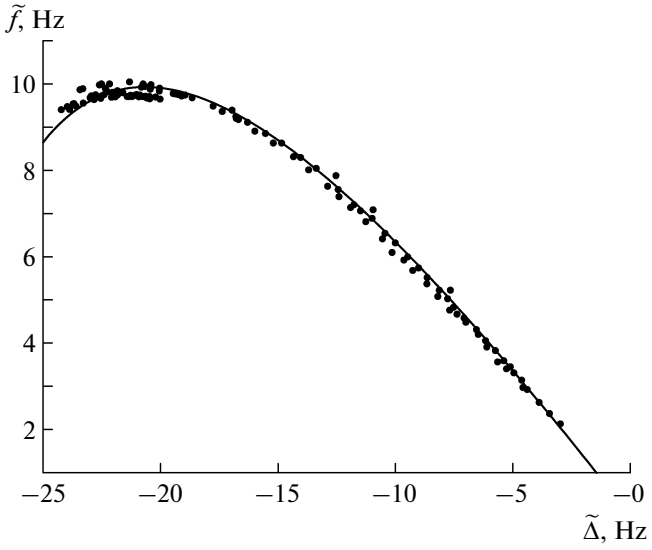

Fig. 8. Dependence $\tilde{f}(\tilde{\Delta})$ according to (5).

for curves *2* and *3* in Fig. 9 averaged over the above temperature range differed by a factor of ~10).

The results presented in curves *1* (Fig. 9) were obtained in a single-cycle experiment with the operating cryostat. The presence of sharp peaks is more pronounced in the dependence $\Delta(T)$. It was established that their appearance is related not to the temperature but to the position of the stratification boundary.

Figure 10 shows the results of measurements in the mode of single-cycle experiments with the same flow rate but different initial amounts of ^{3}He. In this figure, the moments of the disappearance of the upper phase in the dilution chamber, which are registered by an abrupt kink in the dependence $\Delta(t)$, coincide. In the dependences of the resonance-curve width, peaks appear at the same time until the entire process terminates, despite the fact that the readings of the resistance thermometer at the moments when peaks arise are noticeably different. In this case, the presence of peaks obviously cannot be associated with resonances of second sound, whose velocity depends on the temperature; evidently, here we observe first-sound resonances (with a temperature-independent wavelength of ~7.5 mm) in the dilution chamber, whose frequencies are determined by the position of the stratification boundary.

CONCLUSIONS

Measurements of the resonance characteristics of a QTF placed directly in a refrigerant of a dilution refrigerator revealed a number of substantial deviations from the expected smooth temperature depen-

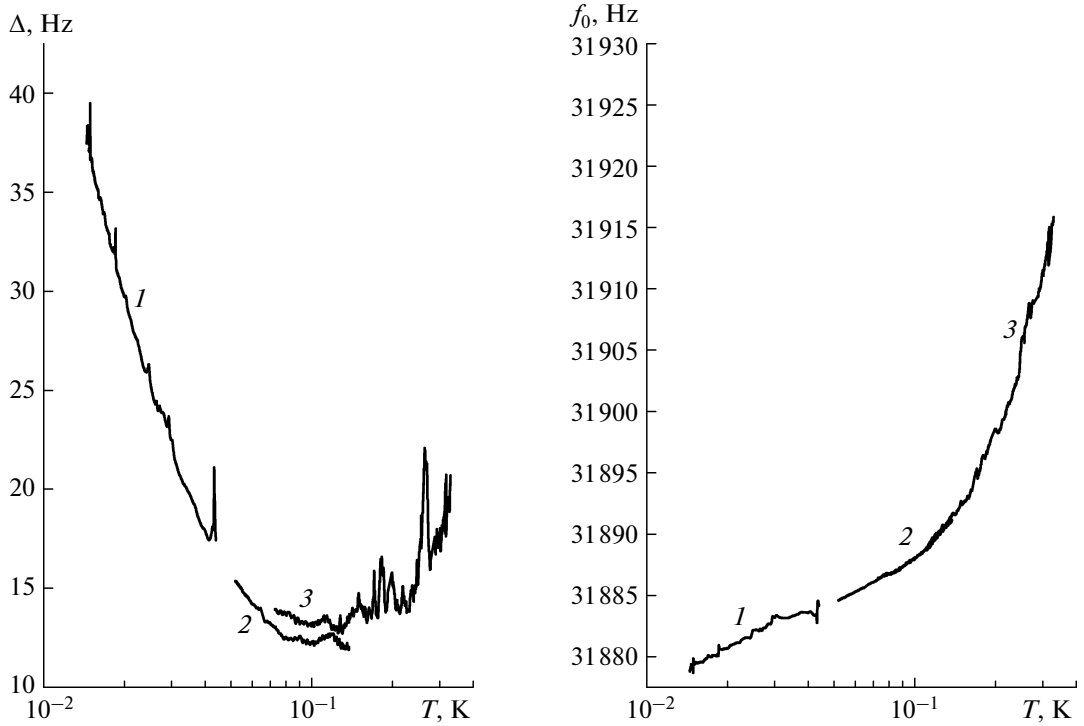

Fig. 9. Temperature dependences of the resonance width and resonance frequency in the diluted phase during cooling: (*1*) in the single-cycle mode, (*2*) with the operating film suppressor in the still, and (*3*) with disabled heaters.

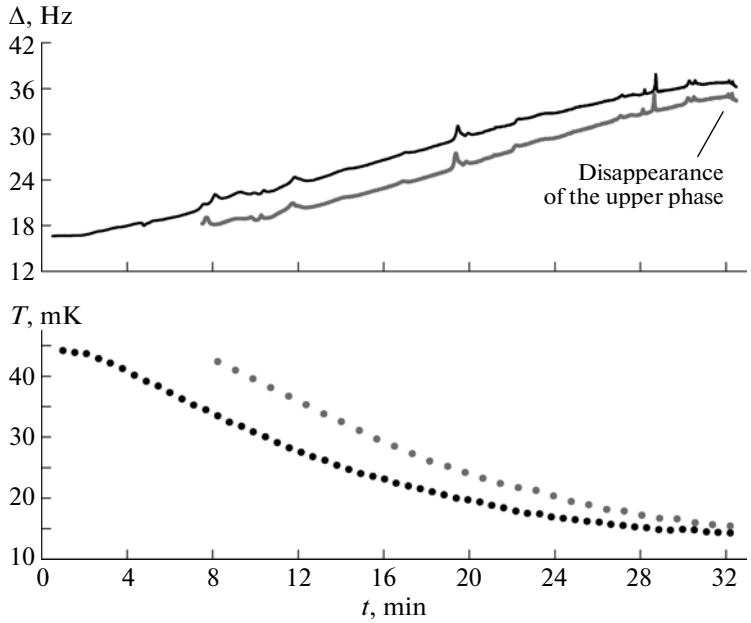

Fig. 10. Time dependences of the widths of the resonance curves and readings of the resistance thermometer in two different the single-cycle modes.

dences of the resonance frequency and width, which are determined by changes in the viscosity and density of the QTF-surrounding medium. When the QTF was placed in different liquid phases in the dilution chamber, deviations had different characters, but in both cases, they correlated with geometrical (the dimensions of the chamber and the QTF itself, its distance to the interphase boundary) and (or) thermal (the rate and direction of temperature changes) characteristics of the instrument and experiment. The physical causes of the appearance of these deviations were discussed above in detail. Note that the existence of deviations leads us to a conclusion that it is undesirable to use a QTF, which is not insulated from a coolant, as a thermometer in a dilution chamber.

ACKNOWLEDGMENTS

We are grateful to V.V. Dmitriev and A.I. Kleev for useful advices and discussions.

This study was supported by the Russian Foundation for Basic Research, project no. 09-02-12200-ofi-m.

REFERENCES

1. Blaauwgeers, R., Blazkova, M., Clovecko, M., et al., *J. Low Temp. Phys.*, 2007, vol. 146, p. 537.
2. Salmela, A., Tuoriniemi, J., Pentti, E., et al., *J. Phys.: Conf. Ser.*, 2009, vol. 150, p. 012040.
3. Blazkova, M., Clovecko, M., Eltsov, V.B., et al., *J. Low Temp. Phys.*, 2008, vol. 150, p. 525.
4. Peshkov, V.P., *Pis'ma Zh.Eksp. Teor. Fiz.*, 1975, vol. 21, no. 6, p. 356.
5. Esel'son, B.N., Ivantsov, V.G., Koval', V.A., et al., *Svoistva zhidkogo i tverdogo geliya. Rastvory $^3He–^4He$* (Properties of Liquid and Solid Helium. ^{3}He–^{4}He Solutions), Kiev: Naukova Dumka, 1982.
6. Esel'son, B.N., Grigor'ev, V.N., Ivantsev, V.G., et al., *Rastvory Kvantovykh Zhidkostei $^3He–^4He$* (Solutions of ^{3}He–^{4}He Quantum Liquids), Moscow: Nauka, 1973.
7. Pobell, F., *Matter and Methods at Low Temperatures*, Berlin: Springer, 2007, p. 28.